William D. Clark

Document Scanner Mechanism

A document scanner mechanism, developed for use in a conventional copier having mirrors which scan a document and reflect the image onto a rotating photoconductor drum, is described in this paper. The engineering design and operation of the mechanism are presented, and the development of an analytical model for simulating its operational characteristics is described, together with the results and conclusions of the simulation. A novel means of generating the scan motion and the important design considerations leading to the development of the scanner mechanism are also presented.

Introduction

The mechanism discussed here was designed for use in a plain paper copier similar to those produced by IBM. These copiers reproduce documents by scanning an illuminated document onto a sheet or panel of light-sensitive material containing an initial surface charge. The document is illuminated and light is reflected by the white background area of the original and focused by a lens onto the light-sensitive panel, causing it to conduct and to discharge the white background areas. This leaves a surface charge on areas corresponding to where dark letters exist on the document. Dry ink particles, charged with opposite polarity to the remaining surface charge of the panel, are used to develop the remaining charge on the panel, thus forming a mirror image of the original. The dry ink is then carefully transferred from the light-sensitive panel to a sheet of copy paper, is fixed by heat, and a copy is made.

In the copier of interest here, the light-sensitive photoconductor (PC) material is wrapped around a rotating cylinder referred to as the PC drum. The document is placed on a flat plane and is scanned by a four-mirror scanning system similar to that used in the IBM Copier II. In the scanning system, illustrated in Fig. 1, the lens is fixed and mirrors are arranged in such a way that the document can be scanned while keeping the distance between the document and the lens constant. The mirrors which scan the document are carried on the first and second carriages. The second carriage moves at half the velocity of the first

carriage, thus keeping the image on the document plane focused on the drum. If the first carriage travels at the same velocity as the surface of the drum, a clear image of the document will be placed on the photoconductor; if it does not travel at that velocity, the image will be blurred because of optical smear caused by position errors between the two.

An imaging lamp is mounted on the first carriage in such a manner that as a document is scanned it is illuminated. If the scanning elements and the drum move at the same but nonconstant velocities relative to the document, some portions of the document may receive more illumination than others, resulting in lighter and darker areas on

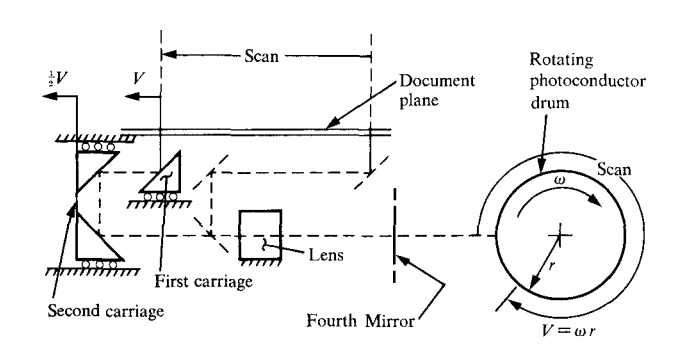


Figure 1 Four-mirror scanning system.

Copyright 1979 by International Business Machines Corporation. Copying is permitted without payment of royalty provided that (1) each reproduction is done without alteration and (2) the *Journal* reference and IBM copyright notice are included on the first page. The title and abstract may be used without further permission in computer-based and other information-service systems. Permission to republish other excerpts should be obtained from the Editor.

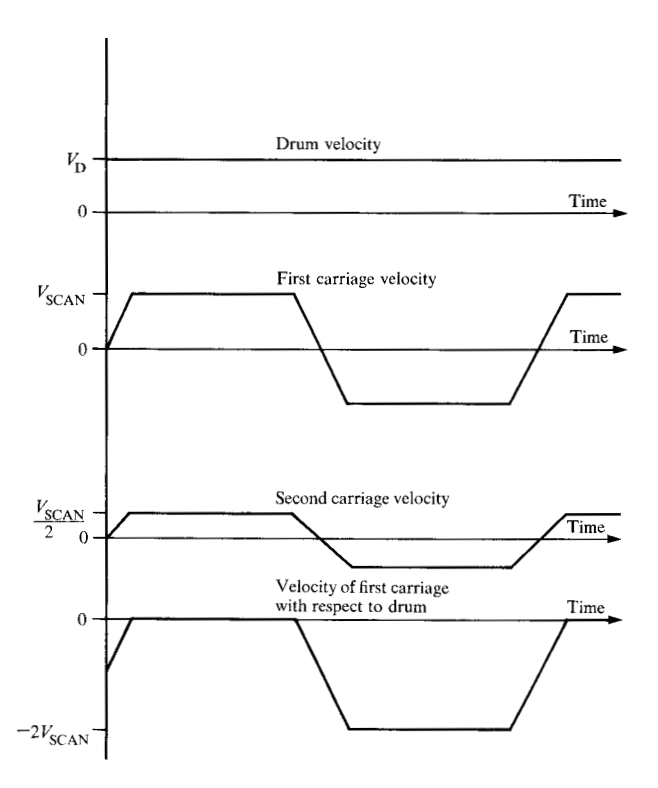


Figure 2 Ideal velocity program.

the copy. Figure 2 shows an ideal velocity program for the system described. Acceleration of the first carriage must be kept low enough to ensure that the lamp filaments are not subjected to excessive acceleration. The relative positions of the first carriage and the drum must be correct to ensure proper registration between the copy and the original document.

All xerographic copy machines which do not flash-expose a document have some means of connecting the scanning optics with the rotating drum. Some of these alternatives will be discussed later in the report. The gear drive and cable drive optics mechanisms, which will be described in additional detail subsequently, are novel means of coupling the rotating drum and the scanning optics.

The first two sections that follow briefly discuss the design requirements for the mechanism and the alternatives that were considered in view of those requirements. The operation of the gear drive and the evolution of its final design are then described in some detail. An analytic model of that design and a discussion of the IBM Continuous System Modeling Program (CSMP) [1], used for simulation, are presented next, followed by the simulation results which led to successful implementation of the

drive. A summary and some conclusions regarding the project are given in the final section.

Requirements

A number of significant design considerations stemmed from several major requirements imposed on the design. The most important of these were motion of the optics, mechanism cost, and serviceability, in addition to meeting specified size and performance characteristics.

• Kinematic requirements

Position accuracy and image growth constaints required that both ends of the image be placed on the photoconductor within 0.1 mm of a reference each time a copy was made.

The absolute velocity variation requirements were constrained by the document illumination. The specific allowable first carriage velocity error was a function of frequency, of PC response, and of aperture width, with five percent a reasonable goal.

The variation of the relative velocity of the photoconductor drum with respect to the scanning optics had to allow imaging at twelve line pairs per millimeter. Specific allowances were a function of frequency; the goal chosen was one percent.

The acceleration goal for the first carriage was 10 m/s². The surface velocity of the drum was approximately 350 mm/s.

• Cost requirement

The cost of the mechanism was to be compatible with low product cost objectives.

• Size requirement

The mechanism had to fit inside a cylinder 150 mm in diameter and 75 mm long. The maximum allowable distance for deceleration at each end of scan was 15 mm.

• Service requirement

In order to facilitate servicing of the mechanism if required, the drive was to be modular with no special tools needed for its replacement.

Alternatives

A number of alternative design choices for the mechanism were considered. In each case, the evaluation criteria used to judge design possibility were how well the particular design would satisfy the requirements heretofore described in regard to position accuracy (0.1 mm), absolute velocity error (5%), relative velocity error (1%), acceleration (10 m/s²), cost (low), and service (modular).

Some of the alternative means used for moving the scanning optics in a copier are listed in Table 1. A cam and linkage similar to that used in the IBM Series III would meet the dynamics requirements, but at a cost considerably greater than the low cost requirement; the same was true for a motor with speed control. A lead screw mechanism would meet all of the requirements except cost. Electric clutches and mechanical dog clutches used in low-cost, low-speed copiers would have unacceptable registration and excessive accelerations when used at scan speeds of 350 mm/s. A combination of cams and clutches as used in the IBM Copier II and as described previously in the IBM Journal of Research and Development [2] would satisfy all the requirements except cost and size.

The gear drive optics mechanism, a novel approach to the scanning optics problem, is the subject of this paper. The description and operation of this mechanism are presented in the next section. Additional details regarding the mechanism may be found in the patent description [3].

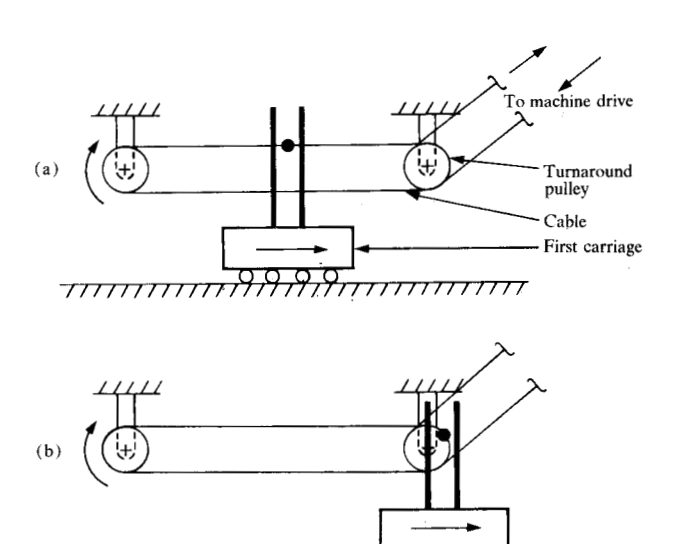
Description of the mechanism

Scotch yoke mechanism

A unique constraint of this scanner application is that the optics scans the document during one drum revolution and then rescans during a second drum revolution. This suggests a modified scotch yoke mechanism, shown in Fig. 3, where the cable is twice the length of the drum circumference and the turnaround pulleys cause the cable and the first carriage to drive at the surface speed of the drum. The cable always drives at constant speed in one direction, and proper attachment of the first carriage to the cable will cause the carriage to move back and forth as shown in Figs. 3(a), (b), and (c). This system has a potential exposure because the cable must be toothed to ensure proper registration. It was felt that the teeth would cause excessive perturbations in the scan velocity.

◆ Cable drive mechanism

To eliminate the exposure of the excessive velocity variations during scan, the cable drive mechanism was proposed. To understand how the drive operates, consider the mechanism of Fig. 3 folded into the arcuate configuration shown in Fig. 4. As indicated in Fig. 4(a), instead of being pulled tight by the turnaround pulleys at the end of scan, the cables are now additionally supported by the idler and drive sprockets which rotate about the drive axis. The oscillating member is constrained to rotate about the drive axis as it is driven by the cable, as shown in Fig. 4(b), and will rotate back and forth around the turnaround pulleys in much the same way as the first carriage reciprocated in Fig. 3.



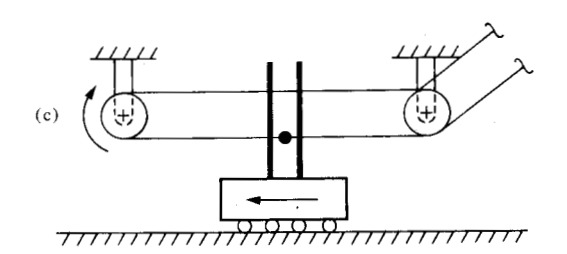
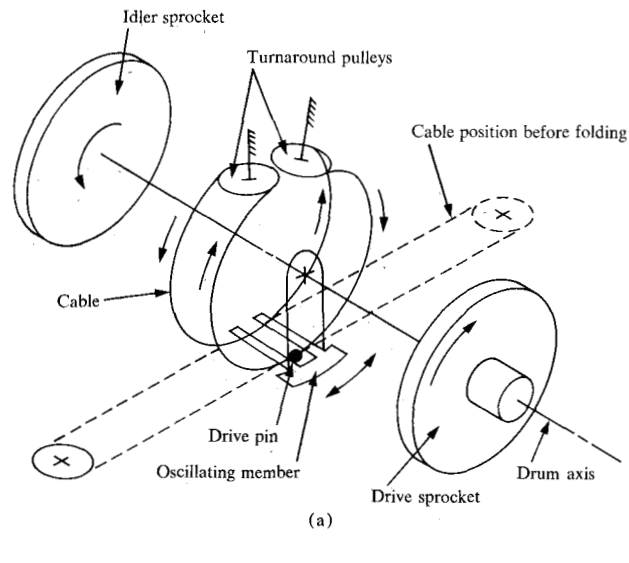


Figure 3 Scotch yoke mechanism: (a) modified mechanism considered here, (b) first carriage near end of rescan, and (c) first carriage scanning.

Table 1 Drive alternatives.

Mechanism	Evaluation		
	Dynamics	Cost	Service
cam and linkage	good	high	good
lead screw	good	moderate	good
motor with speed control	good	high	poor
electric clutches	registration questionable	moderate	good
mechanical clutches	poor	moderate	poor
scotch yoke with belt or chain	questionable	low	good
gear drive mechanism	questionable	low	good

The connection between the cable and the oscillating member is shown in Fig. 5. The oscillating member is connected with the first carriage, so that the optics carriages reciprocate as the pulley oscillates.



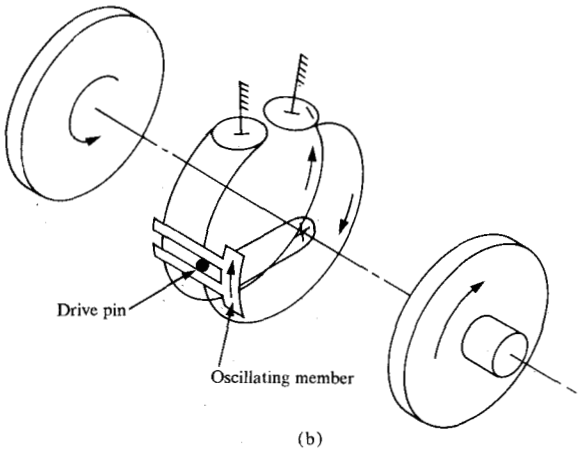


Figure 4 Cable drive mechanism: (a) illustrating cable position before and after folding, and (b) illustrating constraint of motion of oscillating member.

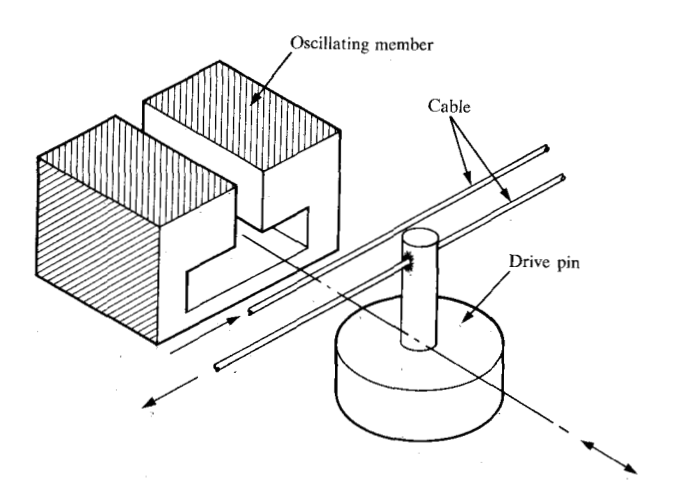


Figure 5 Drive pin and oscillating member.

The configuration of Fig. 4 allows both of the turnaround pulleys to be idlers if one of the sprockets is used to drive the cable. The driving sprocket is rigidly connected to the photoconductor drum so that the two rotate together.

The operation of the cable drive mechanism is briefly as follows. The PC drum rotates constantly in one direction, and as it does, so does the drive sprocket, which is rigidly connected to the drum axis. The drive sprocket causes the cable to move constantly in the arcuate path shown in Fig. 4(b). The cable carries the drive pin with it in its path around one turnaround pulley, the idler sprocket, the other turnaround pulley, and then back to the drive sprocket. When the drive pin is on the drive sprocket side, the oscillating member is turning in the same direction as the PC drum, pulling the scan carriages to properly image the document. When the drive pin is on the idler side, the oscillating member is counterrotating relative to the drum, thereby resetting the scanning optics back to the start of scan.

■ Gear drive mechanism

The configuration shown in Fig. 4 has severe limitations associated with the drive member, the part which was a cable in Figs. 3 and 4. No means can be envisioned which will allow the flexibility required to turn around all the pulleys, to provide the timing required to drive the idler and turnaround pulleys, and at the same time to reliably connect to the oscillating member. The cable is an unacceptable implementation of this concept.

To arrive at the gear drive scan mechanism shown in Fig. 6, the cable was removed, and the drive sprocket, the turnaround pulleys, and the idler sprocket were geared together. The drive gear drives the turnaround gears, which in turn drive the idler gear. Each of the gears has a means of holding the drive pin, allowing the pin to be carried from one gear to the next in the path shown in Fig. 6. The turnaround guide constrains the drive pin when it is in the pockets of the turnaround gears, and the stationary member constrains the drive pin in the pockets of the drive or idler gears.

The drive pin is constrained in the oscillating member in the manner shown in Fig. 5, but without the cable. When the drive pin is in the pocket of the drive gear, the oscillating member rotates in the same direction as the drum, and the optics is scanning. When the drive pin is in either turnaround gear, the oscillating member is decelerating. This situation is similar to what is happening in Fig. 3(b). When the drive pin is in the pocket of the idler gear, the oscillating member is counterrotating relative to the drum and the optics is returning to the start position of the scan.

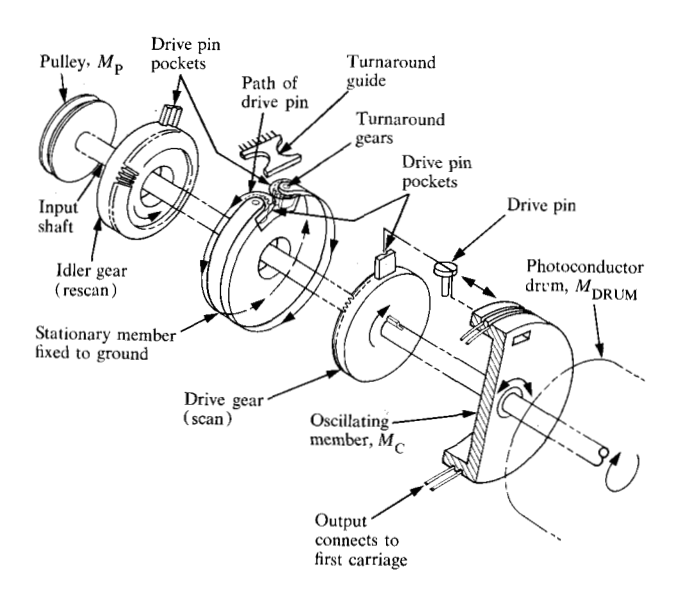


Figure 6 Scan mechanism.

Except for backlash and spring rates present during scan, there is a rigid connection between the input shaft, the scan gear, the drive pin, the oscillating member, and the scan carriages. No motion to the scanning elements is transmitted through the gears. During the rescan, that portion of the cycle when the optics is returning to the starting position, the driving force is transmitted through the gears and the velocity ripple is of no importance.

Mechanism design

After considering the alternatives presented in Table 1, the decision was made to use the gear drive mechanism shown in Fig. 6, since it was compact enough to fit inside the volume allowed, it lent itself to low-cost manufacture, and it could be built in a completely modular manner, resulting in acceptable serviceability.

From a kinematic viewpoint, it appeared that the drive would have acceptable velocity characteristics during the scan. The maximum kinematic acceleration at the turnaround was calculated to be 9.2 m/s when modeled as the scotch yoke mechanism of Fig. 3 with the cable traveling at 350 mm/s around a 13.3-mm-diameter turnaround pulley. However, when backlash, stiffness, and other dynamics are considered, the performance of the gear drive appeared to be questionable.

A mechanism was built and tested to address these concerns, since a simulation was thought impractical at the time because of many unknown spring rates, masses, and backlash conditions in the actual hardware. Figure 7 illustrates typical velocity data taken from the actual hardware and shows a maximum of 16% relative velocity dif-

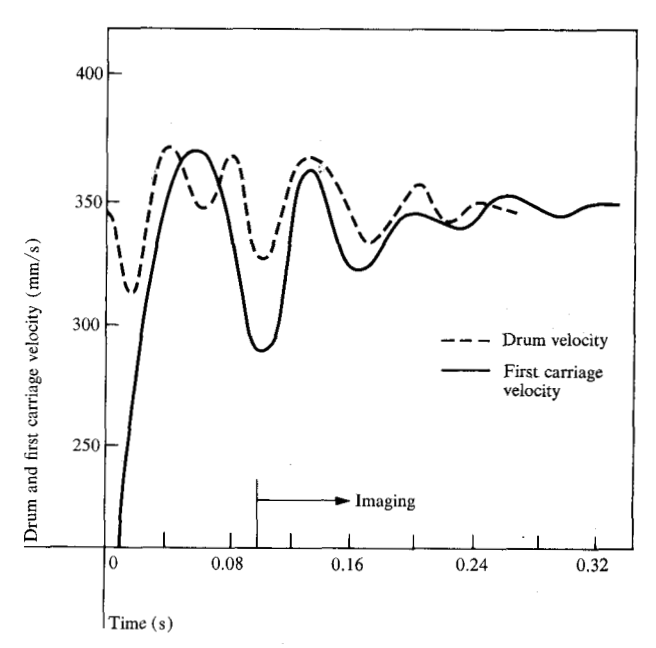


Figure 7 Hardware velocity data.

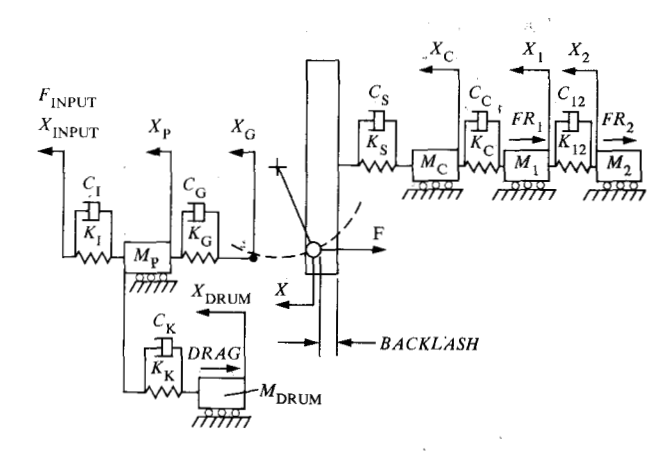


Figure 8 Document scanner lumped mass model.

ference between the drum and the first carriage at 16 Hz, resulting in blurring in the first 50 mm of copy. Zero time in the figure is the center of turnaround. Note that imaging does not start until about 0.1 second after the center of turnaround, allowing some time for oscillations to dampen out. The maximum accelerations were between 1 and 2 g's.

Simulation

• Scan mechanism model and differential equations
To address the exposures in the drive dynamics at the start of scan, the system was modeled on the IBM Continuous System Modeling Program [1]. The lumped mass model of the scanner system is shown in Fig. 8. Rotating

419

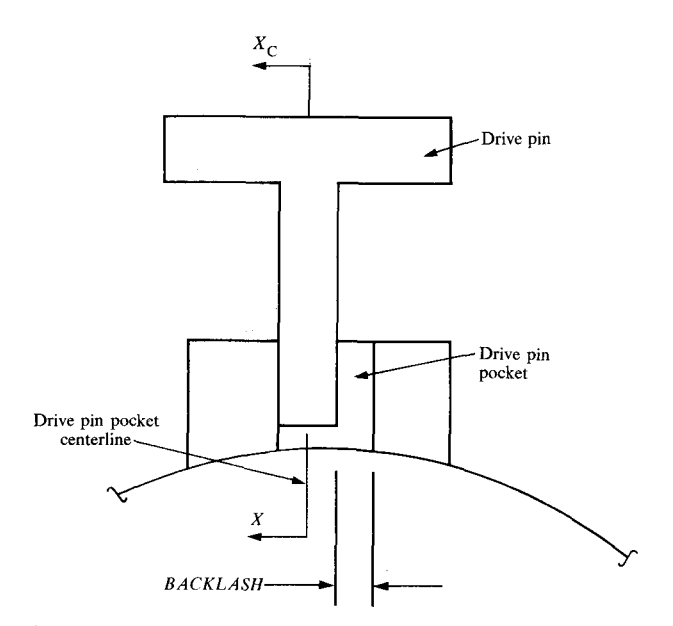


Figure 9 Relation between X, X_{c} , and BACKLASH.

elements and their angular displacements, torques, and moments of inertia have been modeled as translating elements having equivalent position, force, and mass. Symbols are defined in the Appendix.

The applicable differential equations are the following:

$$\begin{split} \ddot{X}_{\rm DRUM} &= \frac{F_{\rm DRUM} - DRAG}{M_{\rm DRUM}}, \\ \ddot{X}_{\rm P} &= \frac{F_{\rm INPUT} - F_{\rm G} - F_{\rm DRUM}}{M_{\rm P}}, \\ \ddot{X}_{\rm C} &= \frac{F - F_{\rm C}}{M_{\rm C}}, \\ \ddot{X}_{\rm I} &= \frac{F_{\rm C} - F_{\rm I2} - FR_{\rm I}}{M_{\rm I}}, \\ \ddot{X}_{\rm 2} &= \frac{F_{\rm I2} - FR_{\rm 2}}{M_{\rm 2}}, \end{split}$$

where the forces are defined as follows:

$$\begin{split} F_{\mathrm{DRUM}} &= K_{\mathrm{K}} (X_{\mathrm{P}} - X_{\mathrm{DRUM}}) + C_{\mathrm{K}} (\dot{X}_{\mathrm{P}} - \dot{X}_{\mathrm{DRUM}}), \\ F_{\mathrm{C}} &= K_{\mathrm{C}} (X_{\mathrm{C}} - X_{\mathrm{1}}) + C_{\mathrm{C}} (\dot{X}_{\mathrm{C}} - \dot{X}_{\mathrm{1}}), \\ F_{\mathrm{12}} &= K_{\mathrm{12}} (X_{\mathrm{1}} - X_{\mathrm{2}}) + C_{\mathrm{12}} (\dot{X}_{\mathrm{1}} - \dot{X}_{\mathrm{2}}), \\ F_{\mathrm{G}} &= K_{\mathrm{G}} (X_{\mathrm{P}} - X_{\mathrm{G}}) + C_{\mathrm{G}} (\dot{X}_{\mathrm{P}} - \dot{X}_{\mathrm{G}}). \end{split}$$

The force between the drive pin and oscillating member, F, is a function of where the oscillating member is in the cycle, that is, rescan, turnaround, or scan; and F also changes depending on the backlash condition of the mechanism existing at the time. In the next section, F is discussed in additional detail. The relation between X,

 $X_{\rm c}$, and *BACKLASH* is illustrated in Fig. 9; this is also discussed in more detail subsequently.

• Function generator

The function generator portion of the model (Fig. 10) simulates the turnarounds between scan and rescan, and backlash. In the model it is assumed that the mechanism is flat, not turned around a cylinder. This results in about 2% error in the position of the optics pulley and less than 5% error in the maximum acceleration during turnaround.

The turnaround section is modeled as shown in Fig. 10(b). The turnaround angle ϕ is related to $X_{\rm G}$ and RE by the relation

$$\phi = \frac{X_{\rm G}}{RE},$$

where X_G is the equivalent arc length around the turnaround gear and RE is the turnaround gear drive pocket radius. The model uses ϕ to determine if the drive pin is in rescan, turnaround, or scan and calculates X from the relations shown in Fig. 10.

A particular problem with modeling the turnaround section is that neither X, the position of the drive pin pocket, nor X_G , the position of the drive gear, has any mass associated with it. If X or X_G had associated mass, the following equations would apply:

$$\ddot{X} = \frac{\Sigma \text{ forces}}{\text{mass}},$$

$$\dot{X} = \int \ddot{X} + C,$$

$$X=\int \dot{X}+C,$$

and X would be available to use in the solution.

Since X and $X_{\rm G}$ do not have any associated mass, they are found indirectly by using the functional relationships to write free body equations around $X_{\rm G}$. These equations are solved for velocity and integrated to find $X_{\rm G}$ and X. It is known from Fig. 8 that

$$F_{\rm G} = K_{\rm G}(X_{\rm P} - X_{\rm G}) + C_{\rm G}(\dot{X}_{\rm P} - \dot{X}_{\rm G}),$$

and tha

$$F = K_{s}(X - X_{c} - BACK) + C_{s}(\dot{X} - \dot{X}_{c}),$$

where BACK is a backlash term to be subsequently discussed. From a free body around $X_{\rm G}$ [Fig. 10(d)], we can write

$$F_{\rm G} = F_{\rm PIN} \sin \phi + F \cos \phi,$$

where $F_{\rm PIN}$ is the sliding friction of the drive pin.

Combining the foregoing equations yields

$$K_{\rm G}(X_{\rm P} - X_{\rm G}) + C_{\rm G}(\dot{X}_{\rm P} - \dot{X}_{\rm G}) = F_{\rm PIN} \sin \phi$$

 $+ [K_{\rm S}(X - X_{\rm C} - BACK) + C_{\rm S}(\dot{X} - \dot{X}_{\rm C})] \cos \phi.$ (1)

Remembering from Fig. 10(b) that

$$X = RE \sin \phi$$
,

then

$$\frac{dX}{dX_{\rm G}} = RE\cos\phi \, \frac{d\phi}{dX_{\rm G}} \, ,$$

and since

$$\phi = \frac{X_{\rm G}}{RE} \,,$$

then

$$\frac{d\phi}{dX_c} = \frac{1}{RE}$$

and

$$\frac{dX}{dX_{\rm G}}=\cos\phi.$$

To find $\dot{X} = f(\dot{X}_G)$, we use

$$\dot{X} = \frac{dX_{G}}{dt} \left(\frac{dX}{dX_{G}} \right) = \frac{dX_{G}}{dt} \cos \phi = \dot{X}_{G} \cos \phi. \tag{2}$$

Substituting Eq. (2) into Eq. (1) yields an equation with one unknown, $\dot{X}_{\rm G}$, all other terms being available in the CSMP solution. Equations (1) and (2) are used in the model to find $\dot{X}_{\rm G}$, which is then integrated with the proper boundary conditions to find $X_{\rm G}$, and X is found from the relations in Fig. 10. During scan and rescan ϕ is set equal to 0 or π .

• Backlash

Gear backlash observed in actual hardware was less than 0.1 mm, and therefore was assumed in the model to be zero. Backlash between the pockets of the gears and the centerline of the drive pin varied between 0 and 1.5 mm and was included (see Fig. 9). The model allowed linear changes in backlash as the drive pin went through rescan, turnaround, and scan. Backlash in the model is treated in the following manner.

A logic routine determines if X is in the backlash region by defining a term $A = X - X_C$ and a dummy term BACK. If $A \le 0$, BACK is zero and X is not in the backlash region. If 0 < A < BACKLASH, then F = 0 and X is in the backlash region. If $A \ge BACKLASH$, then ACK = BACKLASH and ACKLASH and A

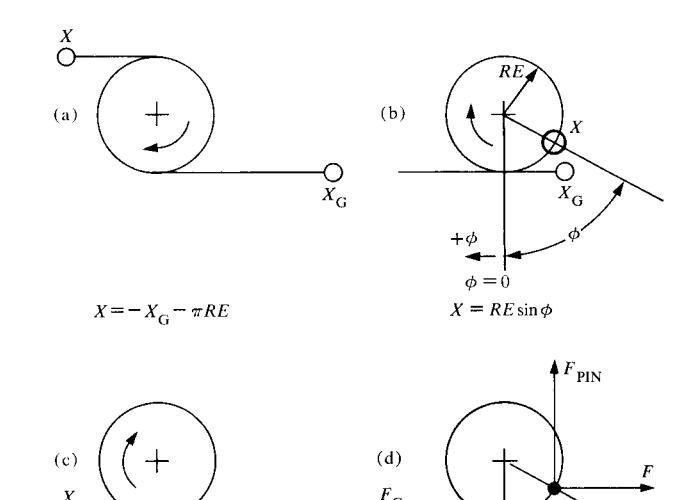


Figure 10 Function generator modeling: (a) rescan section $(\phi < -\pi)$, (b) turnaround section $(-\pi < \phi < 0)$, (c) scan section $(\phi > 0)$, and (d) turnaround forces.

The logic routine determines if X is in the backlash region, and if it is not, Eqs. (1) and (2) are used to solve for X_G . If X is in the backlash region, then F = 0 and Eq. (1) reduces to the following:

$$K_{\rm G}(X_{\rm P}-X_{\rm G}) + C_{\rm G}(\dot{X}_{\rm P}-\dot{X}_{\rm G}) = F_{\rm PIN}\sin\phi.$$

This equation is solved for \dot{X}_{G} and integrated to yield X_{G} .

Simulation results

 $X = X_{G}$

Parameter values necessary for the model were measured on the hardware and entered into the program. Velocity variations at the start of scan predicted by the model are given in Fig. 11. Figure 12 shows the calculated smear results with smear defined as the position of the drum minus the position of the first carriage. The steady state smear is approximately equal to the backlash. It should be noted that steady state smear will appear on a copy as misregistration, not as blurred copy.

Conclusions

After the accuracy of the model was verified, various system parameters were statistically varied to determine which stiffnesses, backlashes, etc. were significant. The simulation results led to the following conclusions:

- 1. Reduction of smear during scan is nearly proportional to the reduction in backlash. See Fig. 12.
- Reduction of friction in the oscillating members had little effect.

421

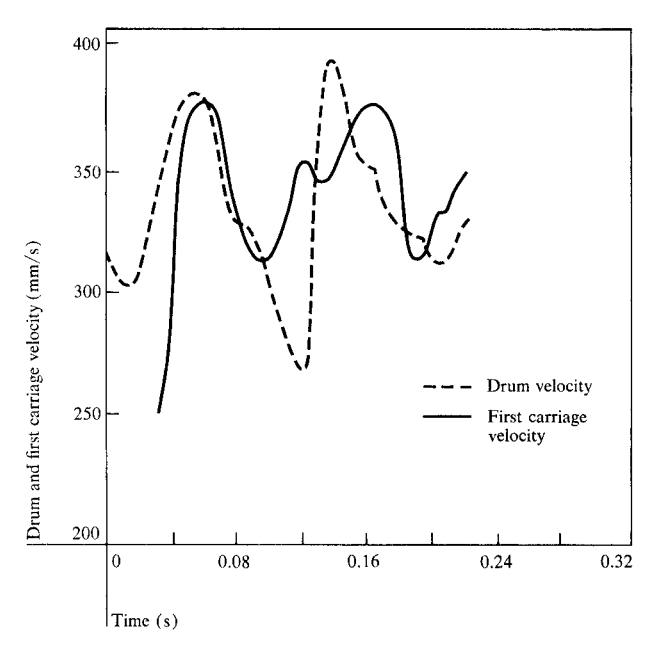


Figure 11 Simulation velocities.

- 3. Increasing the stiffness of the machine drive by a factor of four had no effect on the magnitude of smear. See Fig. 13.
- Reduction of friction in the oscillating members and increased drive stiffness caused the smeared areas to be smaller; that is, the oscillations stopped earlier into scan.

Figure 14 presents data taken from the hardware after the machine drive was stiffened and friction and backlash in the oscillating members were reduced. These improvements allowed the optics to meet the dynamic constraints and the evaluation criteria in all respects. The final result was good copy.

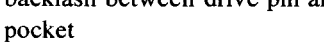
In summary, design requirements of dynamics, cost, and service have been met by the gear drive optics mechanism described herein. The model proved to be a valuable tool in the development stages and gave considerable insight into identifying critical mechanism parameters.

Acknowledgment

The author expresses his appreciation to Norm Cail for development of the computer model of the mechanism.

Appendix: Nomenclature

\boldsymbol{A}	backlash determinate
BACK	dummy backlash variable
BACKLASH	backlash between drive pin and drive pin



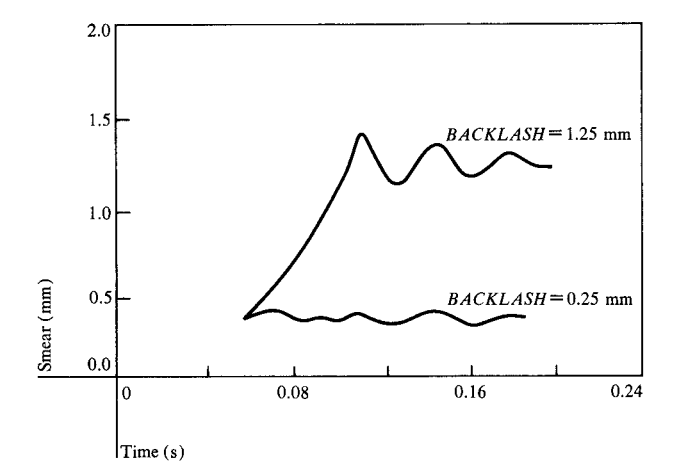


Figure 12 Smear as a function of backlash.

C_{12}	damping between first and second car-
	riage
$C_{ m c}$	damping in cables connecting carriages
	and oscillating member
$C_{ m G}$	gear damping
$C_{\mathfrak{l}}$	input drive damping
$\frac{C_{\rm I}}{C_{\rm S}}$	drive pin damping
$C_{\mathtt{K}}$	drum drive damping
DRAG	drag force on PC drum
F	force between drive pin and oscillating member
F_{12}	force between first and second carriage
$F_{\rm C}$	force between oscillating member and
- 0	first carriage
$F_{ m DRUM}$	force between input drive pulley and the
DRCM	drum
F_{G}	force between the input drive pulley and
•	the drive gear
F_{INPUT}	input force to system
F_{PIN}	sliding friction between oscillating mem-
****	ber and drive pin
FR,	friction between first carriage and ground
FR_{2}	friction between second carriage and
-	ground
K_{12}	spring rate between first and second car-
	riage
$K_{\rm c}$	scan carriage drive cable stiffness
K_{G}	drive gear stiffness
$K_{\rm I}$	input drive spring rate
$K_{\mathbf{K}}$	drum drive spring rate
$K_{\rm S}$	drive pin stiffness
$M_{_1}$	mass of first carriage
M_2	mass of second carriage
$M_{\rm C}$	mass of oscillating member
3.6	CDC 1

mass of PC drum

 $M_{
m DRUM}$

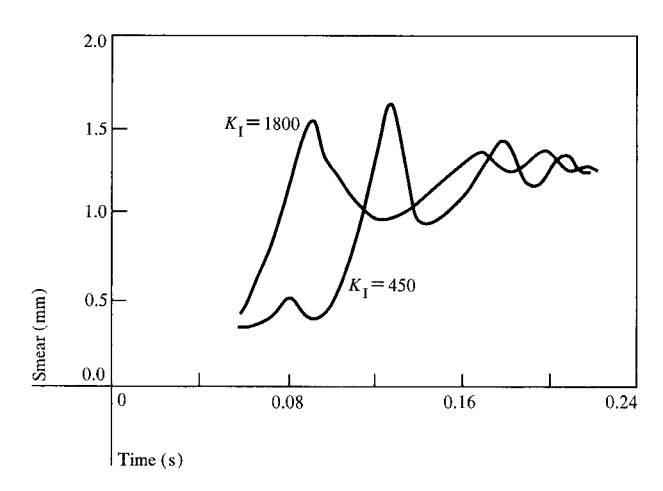


Figure 13 Simulated effect of stiffness on smear.

$M_{ m p}$	mass of machine drive pulley
r	radius of PC drum
RE	turnaround gear drive pocket radius
t	time
V	velocity
$V_{_{ m D}}$	drum surface velocity
$V_{ m SCAN}$	first carriage velocity
X	center of the drive pin pocket
$X_{_{\mathbf{I}}}$	position of the first carriage
X_2	position of the second carriage
$X_{\rm c}$	position of the oscillating member
X_{DRUM}	position of the drum
$X_{ m G}$	position of the drive gear
$X_{ m P}$	position of the input drive pulley
$\boldsymbol{\phi}$	turnaround gear angle
ω	angular velocity of drum

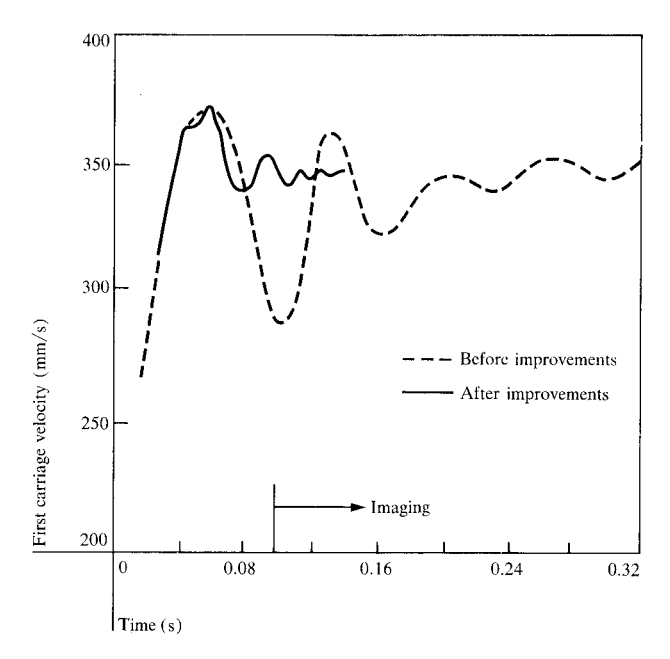


Figure 14 First carriage velocity before and after improvements.

References

- 1. Continuous System Modeling Program III (CSMPIII), Program No. 5734-XS9, IBM Corporation, 1972.
- D. A. Beaty, T. A. Hoskins, T. H. Richards, and H. W. Simpson, "IBM Copier Scanning System," IBM J. Res. Develop. 16, No. 3, 231-238 (1972).
- 3. William D. Clark, "Optics Drive Mechanism," U.S. Patent No. 4,023,897, 1976.

Received November 16, 1978; revised February 25, 1979

The author is located at the IBM Office Products Division laboratory, P.O. Box 1900, Boulder, Colorado 80302.